Biochemical and Biophysical Research Communications 445 (2014) 451–456

Contents lists available at ScienceDirect

Biochemical and Biophysical Research Communications

journal homepage: www.elsevier.com/locate/ybbrc

Crystal structure of cathepsin A, a novel target for the treatment of cardiovascular diseases

Herman A. Schreuder *, Alexander Liesum [1], Katja Kroll [2], Britta Böhnisch [2], Christian Buning [3], Sven Ruf [3], Thorsten Sadowski [4]

Sanofi-Aventis Pharma Deutschland GmbH, Industriepark Höchst, 65926 Frankfurt am Main, Germany

ARTICLE INFO

Article history:
Received 30 January 2014
Available online 12 February 2014

Keywords:
Serine carboxypeptidase
Crystal structure
Heart failure
Drug discovery
Endothelin
Tetrahedral intermediate
Covalent inhibitor

ABSTRACT

The lysosomal serine carboxypeptidase cathepsin A is involved in the breakdown of peptide hormones like endothelin and bradykinin. Recent pharmacological studies with cathepsin A inhibitors in rodents showed a remarkable reduction in cardiac hypertrophy and atrial fibrillation, making cathepsin A a promising target for the treatment of heart failure. Here we describe the crystal structures of activated cathepsin A without inhibitor and with two compounds that mimic the tetrahedral intermediate and the reaction product, respectively. The structure of activated cathepsin A turned out to be very similar to the structure of the inactive precursor. The only difference was the removal of a 40 residue activation domain, partially due to proteolytic removal of the activation peptide, and partially by an order–disorder transition of the peptides flanking the removed activation peptide. The termini of the catalytic core are held together by the Cys253–Cys303 disulfide bond, just before and after the activation domain. One of the compounds we soaked in our crystals reacted covalently with the catalytic Ser150 and formed a tetrahedral intermediate. The other compound got cleaved by the enzyme and a fragment, resembling one of the natural reaction products, was found in the active site. These studies establish cathepsin A as a classical serine proteinase with a well-defined oxyanion hole. The carboxylate group of the cleavage product is bound by a hydrogen-bonding network involving one aspartate and two glutamate side chains. This network can only form if at least half of the carboxylate groups involved are protonated, which explains the acidic pH optimum of the enzyme.

1. Introduction

Cathepsin A, also called human protective protein, is a protein with two very different functions. In its protective function, cathepsin A associates with β-galactosidase and neuraminidase 1 to form a high molecular weight (~700 kDa) multi-enzyme complex [1]. In this complex, β-galactosidase and neuraminidase 1 are protected against lysosomal degradation. In the absence of cathepsin A or with certain cathepsin A mutations, the complex is not formed and β-galactosidase and neuraminidase 1 are rapidly degraded, leading to galactosalidosis [2]. This protective function is independent of the catalytic function, since mice carrying a cathepsin A mutant that is catalytically inactive are still protected against salidosis, although elastic fiber formation and endothelin inactivation were affected [3].

In its catalytic function, cathepsin A is a lysosomal serine carboxypeptidase, which is present in lysosomes, cell membranes and in the extracellular space [4]. It is a member of the α/β hydrolase fold family and its 3-dimensional structure is closely related to those of the homologous wheat serine carboxypeptidase [5], yeast serine carboxypeptidase [6] and hydroxynitrile lyase from *Sorghum bicolor* [7]. The carboxypeptidase activity of cathepsin A has an acidic pH optimum between pH 4.5 and 5.5, but shows deamidase and esterase activities at neutral pH [8] leading to the deamidation of amid-blocked peptides.

* Corresponding author. Address: Sanofi-Aventis Pharma Deutschland GmbH, Building G877, Industriepark Höchst, 65926 Frankfurt am Main, Germany. Fax: +49 6930580169.

E-mail addresses: herman.schreuder@sanofi.com (H.A. Schreuder), alexander.liesum@sanofi.com (A. Liesum), katja.kroll@sanofi.com (K. Kroll), britta.boehnisch@sanofi.com (B. Böhnisch), christian.buning@sanofi.com (C. Buning), sven.ruf@sanofi.com (S. Ruf), thorsten.sadowski@sanofi.com (T. Sadowski).

[1] Sanofi-Aventis Pharma Deutschland GmbH, Building G877, Industriepark Höchst, 65926 Frankfurt am Main, Germany.

[2] Sanofi-Aventis Pharma Deutschland GmbH, Building H812, Industriepark Höchst, 65926 Frankfurt am Main, Germany.

[3] Sanofi-Aventis Pharma Deutschland GmbH, Building G838, Industriepark Höchst, 65926 Frankfurt am Main, Germany.

[4] Sanofi-Aventis Pharma Deutschland GmbH, Building H824, Industriepark Höchst, 65926 Frankfurt am Main, Germany.

http://dx.doi.org/10.1016/j.bbrc.2014.02.014
0006-291X/

Cathepsin A is involved in the breakdown (inactivation) of several bioactive peptides such as endothelin 1 substance P, bradykinin, angiotensin 1 and oxytocin [4] but its exact physiological function is not fully understood. While locally increased bradykinin levels could have a positive effect in cardiac regeneration [9], we discovered novel inhibitors of cathepsin A [10]. Studies in mice with these inhibitors revealed a remarkable reduction in cardiac hypertrophy and atrial fibrillation in heart failure models, pointing to a hitherto unknown pathophysiological role of cathepsin A in cardiac hypertrophy and atrial arrhythmogenesis [10,11].

In addition, cathepsin A has been reported to be involved in the regulation of chaperone-mediated autophagy through the inactivation of the lysosomal receptor Lamp2a [12].

The structure of the 54 kDa inactive cathepsin A precursor was published by Rudenko et al. [13], but here the active site was blocked by the activation domain. During activation, an activation peptide is proteolytically removed, resulting in active protein consisting of a 32 k and a 20 k domain, linked via two disulfide bonds.

In our paper on the discovery of cathepsin A inhibitors [10], we described two crystal structures of cathepsin A–inhibitor complexes. In this paper, we will describe the catalytic mechanism and structure of the activated form of cathepsin A in greater detail, looking at the apo-form, a complex with a covalent inhibitor mimicking the tetrahedral intermediate and a product-like complex.

2. Materials and methods

2.1. Protein purification and crystallization

His-tagged human procathepsin A was expressed in High Five cells and purified by metal-chelate and gel-filtration chromatography as described [10].

2.2. Generation of the active cathepsin A two-chain form by limited proteolysis

The proenzyme was activated by limited proteolysis with cathepsin L or trypsin. Several conditions were tested to obtain the ideal cleavage specificity and speed. Best results were obtained with trypsin immobilized on agarose beads (TPCK treated, Sigma T4019, 27 U/ml) at RT. 5 mg procathepsin A at 0.85 mg/ml was incubated with 0.5 ml equilibrated trypsin-agarose (25 mM Tris pH 8.0, 300 mM NaCl) for 4 h at RT rotating in 10 ml tube at 30 rpm. The reaction was slowed down on ice and the progression of cleavage was monitored on a 4–12% SDS–PAGE. After additional 1 h incubation at RT the trypsin beads were separated by filtration thought a disposable column. Slightly turbid solution was cleared by 5 min centrifugation at 10,000×*g* at 4 °C and passage through a 0.22 μm PVDF membrane filter (Millipore). The presence and integrity of the disulfide bound two-chain cathepsin A was verified on SDS–PAGE using LDS-sample buffer under reducing and non-reducing conditions.

2.3. Crystallography

Cathepsin A was crystallized as described [10] using the hanging drop method: 1 μl of protein solution, containing 6.5 mg/ml cathepsin A, 25 mM Tris–HCl (pH 8.0) and 300 mM NaCl, was mixed with 1 μl reservoir solution, containing 100 mM NaAcetate (pH 4.5), 18–20% PEG400 and 100 mM $CdCl_2$, and set to equilibrate at 4 °C. Rod-shaped crystals appeared in about 1 week. Crystals were soaked with inhibitors by transferring them to a drop of 9 μl reservoir solution with 1 μl of a 100 mM solution of the inhibitor under study in DMSO. For cryoprotection, 20% glycerol was added to the soaking solution and the crystal was picked with a small nylon loop and flash frozen in liquid nitrogen. Data were measured at the ESRF at beam lines ID29 and ID14-4 and processed with XDS/XSCALE [14] as implemented in APRV [15]. The structures were solved using a previously solved cathepsin A structure as a starting model. The initial model was obtained by molecular replacement with Phaser [16] using the cathepsin A precursor structure (pdb code 1IVY; [13]) as a starting model. Model building was done with Coot [17] and refinement was done with Refmac [18] or Buster [19]. No σ cutoff was used during refinement.

3. Results

3.1. Expression, purification and activation of recombinant human procathepsin A

Procathepsin A was expressed by insect cells at good yields around 20 mg/l without degradation or aggregation issues. With a two-step purification a purity of more than 95% could be achieved. The protein was stable after freezing at −80 °C.

However, crystal structures of cathepsin L activated cathepsin A showed an unwanted modification in the active site. To obtain pure and stable mature cathepsin A for crystallization, cleavage with trypsin agarose was employed. For enzyme activation limited proteolysis with immobilized trypsin at near physiological pH yielded the best results in terms of stability, homogeneity, enzyme activity and formation of crystals. The activation procedure results in about 30% yield of mature enzyme from the proenzyme. Analytics showed a homogenous preparation with intact disulfide bridges between the chains of mature cathepsin A.

3.2. Crystallization, structure determination and overall structure

Crystals of cathepsin A diffracted to high resolution (up to 1.6 Å) and the structure was readily solved with molecular replacement using the 1IVY structure as a starting model [13]. Data collection and refinement statistics of the three crystal structures discussed in this paper are given in Table 1.

Whereas procathepsin A crystallized in space group $P2_12_12$ with two molecules in the asymmetric unit, mature Cathepsin A crystallized in space group *C2* with one molecule in the asymmetric unit. In this case, the dimer is formed by two molecules that are crystallographically related. With the exception of the activation domain, most amino acids were well defined in the electron density maps. At the N-terminus, one or two residues of the insect prepromellitin signal sequence were also visible. The edges of the activation domain are not very well defined. Coming from the N-terminus, the electron density around Pro258–Ser259 becomes progressively more disordered, and from around Met299–Asp300 towards the C-terminus, the electron density gets clear again. Blobs of density in between suggest that more residues of the activation loop are still present but not clearly visible due to disorder. At the C-terminus, an extra glutamine is present as leftover from the myc-tag. Here the electron density is very well defined, indicating that the remainder of the myc and His-tags has been cleanly cut during the expression in insect cells.

3.3. Overall structure, based on the 1.6 Å apostructure

Just like the precursor, mature cathepsin A forms a heart-shaped dimer (Fig. 1), which in our case is formed by two crystallographically related monomers. Superposition with the precursor (Fig. 2) reveals that mature cathepsin A is indeed very similar to the precursor with r.m.s. differences in Cα positions of 0.72 Å (412 Cα atoms, monomer A) and 0.64 Å (411 Cα atoms, monomer B) for all equivalent atoms and 0.25 Å (327 Cα atoms, monomer A)

Table 1
Crystallographic data collection and refinement statistics.

Inhibitor	apo	Compound 1	Compound 2
Data collection			
Space group	*C121*	*C121*	*C121*
Cell dimensions			
a,b,c (Å)	90.32 102.03 48.55	90.11 101.29 48.08	89.65 102.53 49.40
α,β,γ (°)	90.00 101.27 90.00	90.00 101.91 90.00	90.00 100.94 90.00
Resolution (A)	33.44–1.58 (1.66–1.58)*	66.25–1.97 (2.07–1.97)*	66.74–1.89 (1.94–1.89)*
$I/\sigma I$	18.1 (2.3)	11.47 (4.12)	14.12 (3.76)
Observed reflctns	185236 (18688)	106951 (9949)	133006 (9779)
R_{meas} (%)	5.1 (47.8)	9.4 (33.3)	9.1 (41.2)
Completeness (%)	96.6 (94.3)	96.2 (73.5)	99.9 (100.1)
Redundancy	3.3 (2.3)	3.7 (3.3)	3.8 (3.8)
Refinement			
Protein atoms	3388	3284	3292
Inhibitor atoms	0	33	14
Water atoms	614	358	911
Other atoms	84	35	61
Resolution (Å)	33.44–1.58 (1.62–1.58)*	36.11–1.98 (2.04–1.98)*	44.02–1.89 (1.94–1.89)*
Reflections used	56890	27298	33271
R_{factor} (%)	16.6 (22.0)	17.3	17.3 (21.5)
R_{work} (%)	16.5 (22.0)	17.0 (26.3)	14.1 (16.5)
R_{free} (%)	19.0 (23.4)	23.2 (33.1)	21.1 (23.6)
Average B-factors (Å^2)			
Protein	19.8	19.3	13.1
Ligand		30.9	16.5
Solvent	39.7	29.6	37.6
Wilson B-fact	17.4	25.0	20.2
Rmsd bond (Å)	0.007	0.014	0.013
Rmsd angles (°)	0.91	1.71	1.41

* The highest resolution bin is given in brackets.

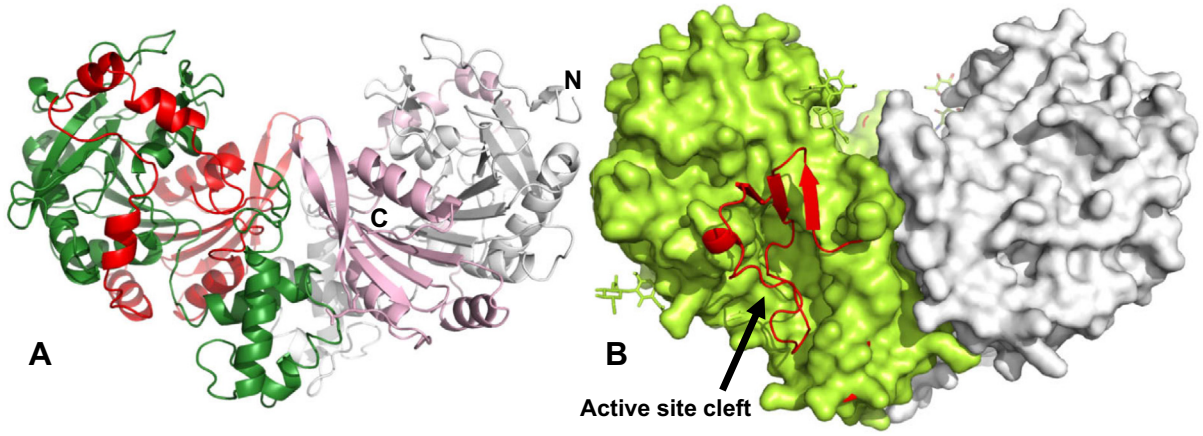

Fig. 1. (A) Cartoon of the cathepsin A dimer built from two crystallographically-related monomers. One monomer is indicated in green (32 k domain) and red (20 kDa domain, the other monomer is indicated in white and pink. (B) Molecular surface of the mature cathepsin A dimer in green and white with a cartoon depiction of the superimposed cathepsin A precursor (pdb code 1ivy; [13]). Clearly visible is how the maturation domain completely fills the active site cleft.

and 0.24 (297 Cα atoms, monomer B) for Cα atoms deviating less than 3σ. The largest differences occur near the beginning and the end of the maturation domain, which has been removed during the activation process. Here the remaining polypeptide chains have moved away from the active site. Two loops around Glu392 and Asp404 have shifted as well. Whereas the loop around Asp404 is solvent exposed and disordered, the loop around Glu392 on the surface of the protein near the dimer interface is well defined. There are no differences in the neighboring residues which could explain the observed differences.

The maturation domain (residues 260–299) is not visible in the electron density maps and has not been modeled. Scattered blobs of electron density in the active site cleft suggest that not the whole maturation domain has been proteolytically removed, but that part of it is still present but disordered. The two termini, before and after the removed/disordered maturation domain, are linked via a disulfide bond, which nicely explains how the maturation domain can be removed without disrupting the rest of the protein structure. Fig. 1B shows how the maturation domain of the precursor structure, completely fills the active site cleft thus preventing any proteolytic activity.

A large active site cleft of ca. 9 Å long and 20 Å wide spans almost the whole width of the cathepsin A monomer (Fig. 1B). The active site itself is a tunnel, which facilitates the displacement of

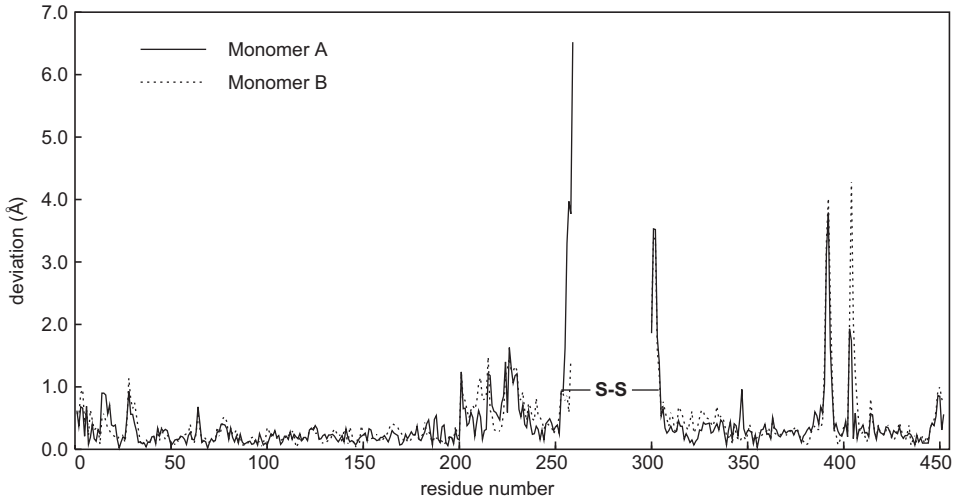

Fig. 2. Deviation in Cα position after superposition of the two independent monomers in the cathepsin A precursor (pdb code 1ivy; [13]) and the single monomer of active cathepsin A (this study). Solid line: monomer A; dotted line: monomer B. Also indicated is the position of the disulfide bond, linking the termini of the 32 k and 20 k domains.

water molecules when the substrate molecule enters the active site. The geometry of the active site and the position of the catalytic residues and the oxyanion-hole will be described in detail in the paragraph about the covalent inhibitor below.

3.4. The structure of the compound 1 complex as a model for the tetrahedral intermediate

One of the screening hits (compound 1) turned out to be a covalent inhibitor of cathepsin A:

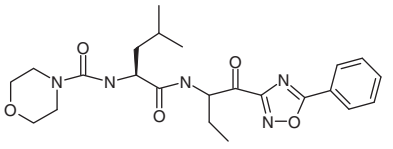

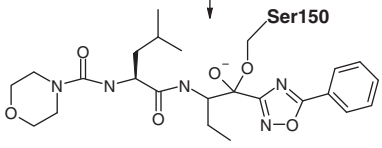

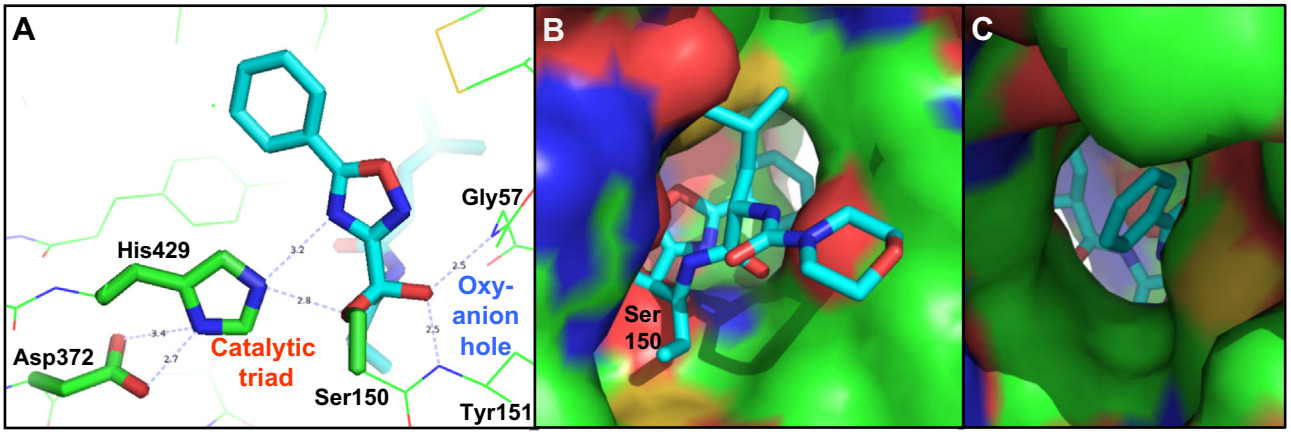

Fig. 3. Binding of compound 1 to cathepsin A. (A). Catalytic machinery of cathepsin A, revealed by the tetrahedral intermediate complex with compound 1. (B) Bound compound 1 (stick model) in the cathepsin A active site (surface representation), viewed from the active site cleft and entrance of the active site tunnel. (C) Bound compound 1, viewed from the exit of the active site tunnel.

The resulting covalent complex (Fig. 3) represents the tetrahedral intermediate as it occurs during catalysis. Fig. 3A clearly shows that Cathepsin A is a classical serine protease with a catalytic triad consisting of Asp372, His429 and Ser150 and an oxyanion hole made by the main-chain nitrogen atoms of Gly57 and Tyr151. The hydrogen bonds, indicated as grey dotted lines have almost perfect geometry, indicative of a highly optimized active site. Interestingly the two hydrogen bonds involving the oxyanion are shorter than usual (2.5 Å), most likely due to the negatively charged oxygen.

The oxadiazole and phenyl groups are located in the tunnel behind the active site, while the ethyl, leucine and morpholino groups are located in the active site cleft. The leucine residue makes multiple van der Waals contacts with Gly57, Pro58, Cys60, Tyr247, Pro301 and Asn339. Its carbonyl oxygen makes a hydrogen bond with the OH of Tyr247 and the nitrogen makes a hydrogen bond with the carbonyl oxygen of Gly57.

The ethyl group makes van der Waals contacts with Gly57 and Cys375 and is located next to the covalent link with Ser150. The morpholino group does not interact with the protein and its electron density is very weak, indicating that it is disordered.

3.5. Cleavage of a ligand: structure of cathepsin A crystals soaked with compound 2

High throughput screening produced a cluster of 33 compounds, the so-called malonamids. One example, compound 2, is shown below:

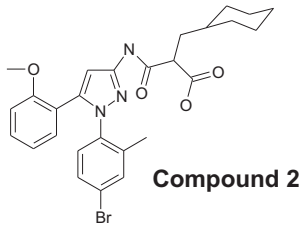

Compound 2 was soaked into cathepsin A crystals and the X-ray diffraction pattern was recorded to 1.9 Å. However, the resulting high-resolution electron density maps only showed density for part of the inhibitor (Fig. 4A). The most likely explanation for this observation is that a fragment of compound 2, which resembles a carboxyterminal amino acid, was cleaved off by the proteolytic activity of cathepsin A:

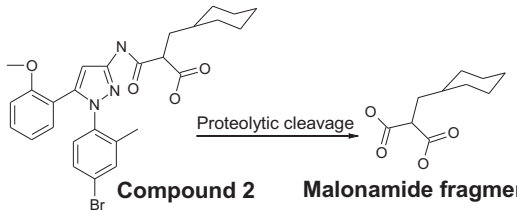

(2)

The fragment remained bound to cathepsin A by nearly perfect hydrogen-bonding network involving the two carboxylate groups (Fig. 4B). This network includes Asn55, Asp64, Glu69, Glu149 and the catalytic residues Ser150 and His429, as well as the main-chain nitrogen atoms of Gly56, Gly57 and Tyr151, of which the latter two form the oxy-anion hole.

This network involves direct hydrogen bonds between four carboxylic acid groups of Asp64, Glu69, Glu149 and the inhibitor. These hydrogen bonds can only exist if at least one of the participating oxygens is protonated. Also, repulsion between deprotonated, negatively charged carboxylates would destroy this hydrogen bonding network. This would happen at non-acidic pH's and provides a nice explanation for the acidic pH optimum of the carboxypeptidase activity of the enzyme.

4. Discussion

The current crystal structures show that the structure of mature cathepsin A is identical to the structure of the precursor and that activation depends solely on the removal/disorder transition of the activation domain. The active catalytic domain is held together by a strategically located disulfide bridge, linking the loose ends that were formed after removal/disorder transition of the activation domain.

Our crystals were grown at acidic pH (4.5) and the formation of a tetrahedral intermediate upon soaking the crystals with compound 1 shows that the protein in the crystals is catalytically active. Also the formation of a cleavage product upon soaking the crystals with compound 2 shows that the protein is active under the conditions used for crystallization. The cyclohexyl "side chain" of the cleavage product fits very well with the preference of the S1' specificity pocket of cathepsin A for hydrophobic residues like leucine, tyrosine and alanine [4].

The presence of a cluster of carboxylate groups (of Asp64, Glu69 and Glu149) in the carboxylate recognition site may allow the

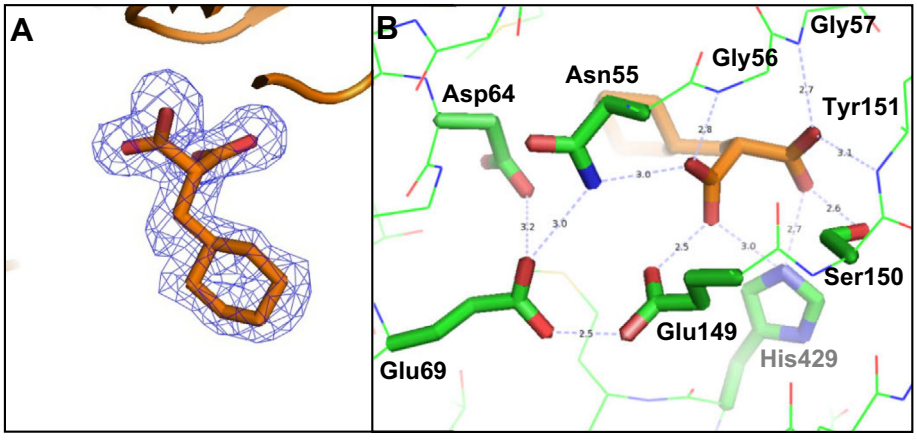

Fig. 4. Binding of compound 2 to cathepsin A. (A) Omit electron density observed after soaking a cathepsin A crystal with compound 2. (B) Hydrogen bonding network around the two carboxylate groups of the malonamide fragment.

switch from carboxylase activity at acidic pH with neutral carboxylates and an intact carboxylate recognition site, to deamidase activity at neutral pH, when the carboxylate recognition site is disrupted due to repulsion of the now negatively charged carboxylate groups.

Also a second effect, put forward by Bullock et al. [20], based on the structure of the complex of benzylsuccinate with wheat serine carboxypeptidase II, may play a role with cathepsin A as well: At acidic pH, the catalytic histidine is most likely fully protonated, making it impossible to accept a proton from the catalytic serine either just before or during the nucleophilic attack of this serine on the substrate carbonyl group. In our structure of the complex with the cleavage product, as in the structure of the very similar benzylsuccinate complex by Bullock et al., the carboxylate group, corresponding to the carboxy-terminal carboxylate group of peptide substrates, is hydrogen bonded to the catalytic histidine and could accept a proton from this histidine during catalysis, which would allow catalysis to proceed at acidic pH's. In case of amidated substrates, the amidated carboxylate group is not able to accept a proton from the histidine, shifting the optimum pH for the reaction to neutral or basic pH, as is normally observed for serine proteinases.

The position of the catalytic site at the entrance of the active site tunnel perfectly explains the observed carboxypeptidase (exopeptidase) activity of cathepsin A and lack of proteinase (endopeptidase) activity observed in an FITC-casein proteinase assay [21]. More difficult to explain, however, is the endopeptidase activity proposed to occur during the degradation of lamp2a [12]. Here the polypeptide chain of lamp2a gets cleaved between the luminal and transmembrane domains by a membrane-associated form of cathepsin A. In this case one has to assume that either cathepsin A undergoes some conformational change upon membrane association (possibly with opening of the 253–303 disulfide link), or that the lamp2a chain adopts a sharply bent conformation, which allows it to bind to the cathepsin A active site, which would normally not accept residues beyond P1′. More studies will be necessary to solve this issue.

Accession numbers

Coordinates and structure factors have been deposited in the Protein Data Bank with the accession numbers 4ci9, 4cia, and 4cib.

References

[1] M. Potier, L. Michaud, J. Tranchemontagne, L. Thauvette, Structure of the lysosomal neuraminidase-β-galactosidase-carboxypeptidase multienzymic complex, Biochem. J. 267 (1990) 197–202.
[2] A. D'Azzo, A. Hoogeveen, A.J.J. Reuser, D. Robinson, H. Galjaard, Molecular defect in combined β-galactosidase and neuraminidase deficiency in man, Proc. Natl. Acad. Sci. USA 79 (1982) 4535–4539.
[3] V. Seyrantepe, A. Hinek, J. Peng, M. Fedjaev, S. Ernest, Y. Kadota, M. Canuel, K. Itoh, C. Morales, J. Lavoie, J. Tramblay, A.V. Pshezehetsky, Enzymatic activity of lysososmal carboxypeptidase (cathepsin) A is required for proper elastic fiber formation and inactivation of endothelin-1, Circulation 117 (2008) 1973–1981.
[4] M. Hiraiwa, Cathepsin A/protective protein: an unusual lysosomal multifunctional protein, Cell. Mol. Life Sci. 56 (1999) 894–907.
[5] D.-I. Liao, K. Breddam, R.M. Sweet, T. Bullock, S.J. Remington, Refined atomic model of wheat serine carboxypeptidase II at 2.2-Å resolution, Biochemistry 31 (1992) 9796–9812.
[6] J.A. Endrizzi, K. Breddam, S.J. Remington, 2.8-Å structure of yeast serine carboxypeptidase, Biochemistry 33 (1994) 11106–11120.
[7] H. Lauble, B. Miehlich, S. Förster, H. Wajant, F. Effenberger, Crystal structure of hydroxynitrile lyase from *Sorghum bicolor* in complex with the inhibitor benzoic acid: a novel cyanogenic enzyme, Biochemistry 41 (2002) 12043–12050.
[8] H.L. Jackman, P.W. Morris, P.A. Diddish, R.A. Skidgel, E.G. Erdös, Inactivation of endothelin I by deamidase (lysosomal protective protein), J. Biol. Chem. 267 (1992) 2872–2875.
[9] D. Westermann, H.-P. Schultheiss, C. Tschöpe, New perspective on the tissue kallikrein-kinin system in myocardial infarction: role of angiogenesis and cardiac regeneration, Int. Immunopharmacol. 8 (2008) 148–154.
[10] S. Ruf, C. Buning, H. Schreuder, G. Horstick, W. Linz, T. Olpp, J. Pernerstorfer, K. Hiss, K. Kroll, A. Kannt, M. Kohlmann, D. Linz, T. Hübschle, H. Rütten, K. Wirth, T. Schmidt, T. Sadowski, Novel β-amino acid derivatives as inhibitors of cathepsin A, J. Med. Chem. 55 (2012) 7636–7649.
[11] S. Ruf, C. Buning, H. Schreuder, W. Linz, T. Hübschle, D. Linz, H. Ruetten, K. Wirth, T. Sadowski, Inhibition of CatA: an emerging strategy for the treatment of heart failure, Future Med. Chem. 5 (2013) 399–409.
[12] A.M. Cuervo, L. Mann, E.J. Bonten, A. d'Azzo, J.F. Dice, Cathepsin A regulates chaperone-mediated autophagy through cleavage of the lysosomal receptor, EMBO J. 22 (2003) 47–59.
[13] G. Rudenko, E. Bonten, A. d'Azzo, W.G.J. Hol, Three-dimensional structure of the human 'protective protein': structure of the precursor form suggests a complex activation mechanism, Structure 3 (1995) 1249–1259.
[14] W. Kabsch, XDS, Acta Crystallogr. D66 (2010) 125–132.
[15] M. Kroemer, M.K. Dreyer, K.U. Wendt, *APRV* – a program for automated data processing, refinement and visualization, Acta Crystallogr. D60 (2004) 1679–1682.
[16] A.J. McCoy, R.W. Grosse-Kunsleve, P.D. Adams, M.D. Winn, L.C. Storoni, R.J. Read, *Phaser* crystallographic software, J. Appl. Crystallogr. 40 (2007) 658–674.
[17] P. Emsley, K. Cowtan, Coot: model-building tools for molecular graphics, Acta Crystallogr. D60 (2004) 2126–2132.
[18] G.N. Murshudov, P. Skubák, A.A. Lebedev, N.S. Pannu, R.A. Steiner, A. Robert, R.A. Nicholls, M.D. Winn, F. Long, A.A. Vagin, REFMAC5 for the refinement of macromolecular crystal structures, Acta Crystallogr. D67 (2011) 355–367.
[19] G. Bricogne, E. Blanc, M. Brandl, C. Flensburg, P. Keller, W. Paciorek, P. Roversi, A. Sharff, O.S. Smart, C. Vonrhein, T.O. Womack, BUSTER, Global Phasing Ltd., Cambridge, United Kingdom, 2011.
[20] T.L. Bullock, B. Branchaud, S.J. Remington, Structure of the complex of L-benzylsuccinate with wheat serine carboxypeptidase II at 2.0-Å resolution, Biochemistry 33 (1994) 11127–11134.
[21] J.J. Miller, D.G. Changaris, R.S. Levy, Purification, subunit structure and inhibitor profile of cathepsin A, J. Chromatogr. 627 (1992) 153–162.